IEEE Access
Multidisciplinary ⋮ Rapid Review ⋮ Open Access Journal

Received November 29, 2021, accepted December 4, 2021, date of publication December 20, 2021,
date of current version January 5, 2022.

Digital Object Identifier 10.1109/ACCESS.2021.3137092

Locational Tariff Structure for Radial Network Fixed Costs in a DER Context

VERONICA S. ETCHEBEHERE[1] AND JOSÉ W. MARANGON LIMA[2], (Senior Member, IEEE)
[1]Department of Electricity, Federal University of Amazonas (UFAM), Manaus 69077-000, Brazil
[2]Department of Electrical Engineering, Federal University of Itajubá (UNIFEI), Itajubá 37500-903, Brazil

Corresponding author: Veronica S. Etchebehere (vetcs@ufam.edu.br)

ABSTRACT The regulation of Distributed Energy Resources (DERs) has cast doubt on the sustainability of utility infrastructure charging models. The development of feed-in tariffs, net-metering, and network charge rebates for distributed generation (DG) has been questioned because of the cross-subsidies that result between passive consumers and DG investors. Besides DG investors, other new entrants, such as owners of energy storage resources and electrical vehicles, are creating challenges for the regulation of distribution service pricing as a whole. This paper proposes a new approach to dealing with the fixed cost element of service pricing, that enhances economic signaling in the distribution network. We isolate and address the issue from a distribution network point of view, by excluding from our model the random variables associated with the complexity of social, environmental and other externalities. The solution developed is particularly relevant at a time when distribution networks, historically dominated by passive users, struggle to adapt to a dramatic increase in the number of users who are active agents. It considers the principles governing tariff design from the perspective of simplicity, economic signaling, and revenue reconciliation. Results are presented of simulations performed with different arrangements of alternative energy generators and energy storage devices, using an actual feeder from a distribution company in Brazil. An analysis of these results is provided that suggests a combination of locational and time-of-use rates can provide effective economic signals to these new types of system user.

INDEX TERMS Distributed energy resources, distributed generation, locational tariffs, network pricing.

I. INTRODUCTION

In contrast to other countries where feed-in tariffs have been applied, Brazil introduced net-metering in 2012, through Resolution 482 of the Brazilian National Electrical Energy Agency (ANEEL) [1]. This resolution has influenced the Brazilian energy market, particularly the solar energy segment, which was effectively non-existent before 2012, but which had grown to 5GW installed capacity by 2020 [2]. However, the policy calls into question the sustainability of a utility business model based exclusively on energy volumetric price. For low-voltage (LV) consumers, monomial rates are designed to recover all energy consumption and infrastructure costs. However, the current system of tariff compensation for Distributed Energy Resources (DERs) negatively impacts a utility's revenue stream by generating discounts for prosumers without accounting for cost causality. This disconnection between rate structures and fixed costs is undesirable, and represents a major challenge for regulators.

It is common sense that users who contribute to the energy flow at the distribution network must pay for its use, whether or not they are generators or loads. However, finding a tariff structure that is coherent with the new operating reality of distributed systems is not a simple task. Distribution systems are complex, and energy flows are highly nonlinear. Besides, most new investors in distributed generation are in fact erstwhile consumers who have become active agents in the electrical grid.

In evaluating any methodology, it is appropriate to take as a starting point the basic principles governing tariff structure [3], [4]. A sustainable tariff should have the attributes of economic efficiency, equity, and revenue stability, in addition to being consumer-friendly through simplicity of concept and consistency over time. Tariff design should incorporate network charges, and tariffs should function as commercial instruments that positively influence user behavior by promoting the most efficient usage of the network. Finally,

The associate editor coordinating the review of this manuscript and approving it for publication was Ehab Elsayed Elattar.

a tariff needs to promote a fair allocation of costs across different consumer profiles.

There are essentially two types of network infrastructure cost, namely: (a) costs of the existing system (or fixed costs); and (b) costs of network congestion and losses - i.e. those costs used in incremental pricing models. Fixed cost pricing is designed to recover all asset costs over time, while incremental pricing produces economic signals for agents of the system, with respect to their network usage. According to [5], only a combination of *both* pricing methods can hope to effectively incorporate cost recovery and effective signaling.

There is an increased interest in tariff models that address the issue of congestion costs in distribution networks. Several methods have been proposed, including methodologies based on dynamic tariffs [6], [7], distribution locational marginal price [8]–[10], and social welfare maximization [11]. Reference [12] proposed a composite method incorporating locational marginal price and either a postage-stamp or marginal participation element.

Despite the importance of incremental pricing, regulators remain focused on the design of tariffs for the attribution and recovery of distribution network fixed costs. Due to the high value of these fixed costs, it is important to allocate them correctly based on individual network usage patterns. The MW-mile method and its variations [13] are widely used for fixed cost attribution in transmission networks. In distribution systems, the MW-mile was used by [14], [15], while in [16], the Amp-mile (a sensitivity matrix method based on absolute current values) is used to determine an agent's usage of distribution network circuits. In [17], the authors suggested a tariff based on the topological model developed by [18], with the MW-mile method used to apply the charge. In [19] analytical expressions were used to map the contribution of power injections to the branch in an AC network. In [20] and [21] the authors developed two mathematical models to charge net users based on a system impedance matrix Z_{bus} - one model for the apportionment of losses, and another for network fixed costs. The authors concluded that this method would encourage a better agent distribution across the network. Another model [22], compared the Z_{bus} allocation method with existing charging models. In [23], costs were attributed using a game theory model. Finally, in [24], the authors created a bilevel optimization tariff model based on the interaction between the system operator and users.

In our case, we establish a fixed-cost pricing approach to the radial distribution problem that considers both locational and time-of-use drivers in the tariff structure. Sensitivity matrices are used to assess user impact, and different variations of the MW-mile apportionment model are applied to identify which one is most appropriate. We also consider whether - and if so, how - the presence of a postage-stamp element can influence economic signaling.

We chose absolute current value over active power in determining system usage. A new current sensitivity matrix is used for allocating losses among system users. The methods are then tested by using an actual distribution feeder with residential, commercial, and industrial consumers.

The rest of this paper is organized as follows: Section II presents the proposed methods and their modification to accommodate a variety of distributed generation and demand responses. Section III introduces our proposed system and the simulation process. Sections IV and V provide results and a discussion. Finally, Section VI draws a conclusion.

II. PROPOSED METHODS

The tariff structure for LV consumers is usually volumetric, which has led to increasing concerns about the allocation of distribution charges among consumers and prosumers. However, if it incorporates appropriate time-of-use and locational elements, a tariff structure can contribute to the efficient allocation and operation of PVs and energy storage resources.

We propose allocation methods that use absolute current values rather than active power values, and that are better adapted to radial system characteristics. To determine the tariff of each user (facility) in the network, variants of the MW-mile allocation strategy presented by [13], were tested to find the more appropriate model.

Since active and reactive power ($P = VI\cos\varphi$ and $Q = VI\sin\varphi$, respectively), have a direct relationship with absolute current value, we chose to use the proportional property of the current for tariff calculation. In addition, as in [16], distribution networks were designed primarily to handle circuit currents within the thermal capacity limits of a circuit.

Our proposed model is based on the calculation of the flow in each circuit caused by the generation/load pattern of each agent, using the OpenDSS AC power-flow model. This program simulates n-phase load-flow using a set of direct equations based on the system's nodal admittance matrix [25]. Each agent's system usage is then determined by calculating a sensitivity matrix (Section A, below). Finally, the tariff is calculated based on a proportional sharing principle using one of three apportionment models (Section B). Section C presents the loss apportionment calculation using a loss sensitivity matrix. Fig. 1 shows the simulation flow chart.

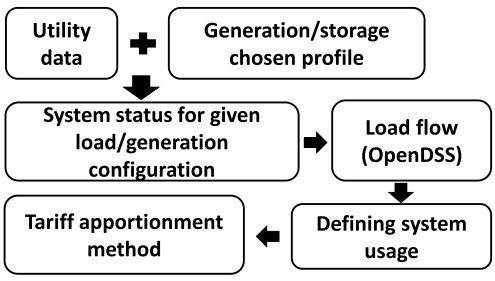

FIGURE 1. Simulation flow chart.

A. APPROACH TO DEFINING SYSTEM USAGE

The proposed approach is an adaptation of the Amp-mile model which uses Power-to-Current Distribution Factors (PCDFs) as a measure of consumer usage of the

network [16]. This model, using analytical calculation to derive a sensitivity matrix, has a lower computational cost than those using empirical methods.

Two different sensitivity matrices are used: one for circuit flow; and another for losses. For circuit flow, the calculation of the derivatives is based on the Amp-mile method, but considers the relationship between line and node currents (see appendix, section A) as in (1) below. The line currents were considered to be the sum of all loads/generations at each node. In addition, in contrast to the Amp-mile model, we used the absolute values of the sensitivity matrix, limiting circuit flow tariffs to positive values.

$$DF_{lk}^{t} = \left| \frac{\partial |I_l^t|}{\partial |I_k^t|} \right| \tag{1}$$

Here, DF_{lk}^{t} is the absolute value of the current-to-current distribution factor between line l and node k, at time t. $\left|I_l^t\right|$ is the absolute value of line l current, at time t, and $|I_k^t|$ is the absolute value of node k current, at time t.

It is important to note that the Jacobian matrix is designed to deal with both the active and reactive elements of the line currents. The matrix is composed of four sub-matrices (H, L, M, N), where matrices M and N are zero matrices and H and L are matrices of the partial derivative of the modulus of the node current.

$$[J]_{2L\times 2L} = \begin{bmatrix} H_{L\times L} & 0 \\ 0 & L_{L\times L} \end{bmatrix} \tag{2}$$

where $[H] = \partial F/\partial I$ is the absolute value of the current-to-current distribution factor between line l and node k, coming from the active part of the line current; and, $[L] = \partial F/\partial I$ coming from the reactive part of the line current. The final Jacobian matrix derives from the multiplication of intermediate Jacobian matrices, as detailed in the appendix.

The sum of the contributions of each line l to node k of H and L provide the final user tariff at node k, reflecting the active and reactive consumption of all users.

With respect to the loss apportionment calculation, in [20] the authors presented (3) for power loss allocation calculus. They then used the equation directly for tariff design. Our approach, however, calculates the sensitivity matrix using (3) to develop the allocation method (see appendix, section B):

$$P_{loss}^{t} = \Re \left\{ \sum_{k=1}^{n} \left(I_k^*\right)^t \cdot \sum_{j=1}^{n} R_{kj} I_j^t \right\} \tag{3}$$

where P_{loss}^{t} is the power loss at time t, I_k^t is the current at node k at time t, and n is the number of nodes in the circuit. R is the real element of the system impedance matrix.

The use of the real element of the impedance matrix is considered desirable, since it reflects the electrical distance between nodes [20], [21], and the locational effect in the tariff is thus achieved. In addition, real values of the sensitivity matrix were used for loss apportionment, instead of absolute values. The rationale for this is that losses are also valued in terms of energy, and any loss reduction is beneficial to all feeder users.

DLF_k^t is the loss-to-current distribution factor for node k, at time t:

$$DLF_k^t = \frac{\partial P_{loss_k}^t}{\partial |I_k^t|} \tag{4}$$

where $P_{loss_k}^t$ is the loss in node k, at time t, and $\left|I_k^t\right|$ is the absolute value of node k current, at time t.

Finally, LPC_k^t represents the loss proportionality constant for the apportionment of electrical losses in node k, at time t:

$$LPC_k^t = \frac{DLF_k^t}{\sum_{i=1}^{n} DLF_i^t} \tag{5}$$

B. TARIFF APPORTIONMENT METHOD

The tariffs were calculated using the Zero Counterflow Method (ZCFM) and the Dominant Flow Method (DFM), as first described in [13]. The main difference in our model is the use of absolute current value instead of the value of the active power.

As with the ZCFM model, in our approach the tariff is calculated in such a way as to avoid a locational charge on the agent whose power flow is opposite to the direction of the net flow. We consider that the generator or prosumer would be compensated (or would not pay) when there is a reduction in the line load, or charged when they cause an inversion in the flow. The tariff changes every hour depending on load/generation pattern. For this reason, a logical condition for the application of the tariff was added to the apportionment models, such that a charge is generated only to agents that satisfy that logical condition. The added condition is that the real part of the relationship *node current to line current* must be greater than zero (when $R\{I_k/I_l\} > 0$). In the unlikely case of a charge being purely reactive, it is considered neutral, since it does not contribute to the flow of active power. In this case, the agent does not pay a locational tariff element.

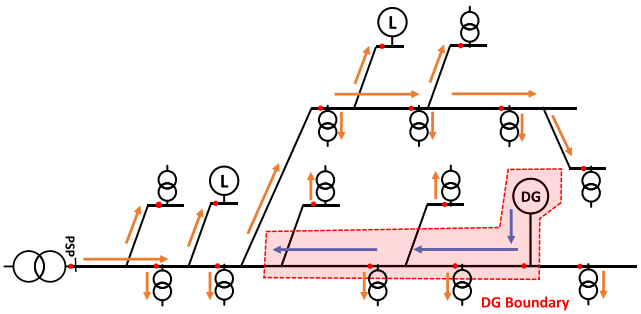

FIGURE 2. DG module boundary example.

The tariff is designed to account for DG module energy boundaries, i.e. where a DG module's energy inverts the net flow in the feeder (Fig. 2). It thus assumes that any reduction in the net flow is beneficial. There is no locational charge for a user who relieves the circuit flow. The prosumer pays more

for network usage when they cause current flow inversion, and receives a discount if their presence relieves the flow.

1) THE ZERO COUNTERFLOW AMP MODEL (ZCAM)

The ZCAM is derived from the ZCFM, and provides for the recovery of all embedded costs. With this method, there is no charge to the agent whose current flow is in the opposite direction to the net flow.

This model does not assume that system reserve benefits everyone. The model for the locational tariff, LT is:

$$\begin{cases} LT^t_{ZCAM_k} = |I^t_k| \sum_{l=1}^{m} \left(\dfrac{1}{|I^t_l|^{s+}} \right) \\ \qquad \cdot CC^t_l \cdot DF^t_{lk} \quad when\ \Re\{\dot{I}^t_k/\dot{I}^t_l\} > 0 \\ LT^t_{ZCAM_k} = 0 \qquad when\ \Re\left\{\dot{I}^t_k/\dot{I}^t_l\right\} \leq 0 \end{cases} \tag{6}$$

where I^t_k is the current at node k at time t. CC^t_l is the circuit cost of load element of the branch l, and $\left(I^t_l\right)^{s+}$ is the sum of current positive flows from users in branch l, at time t. The number of lines in the distribution network is m.

2) THE DOMINANT AMP MODEL (DAM)

The DAM is derived from the DFM. It assumes that any flow reduction is beneficial to the system, and, at the same time, distributes the full cost of the capacity of the system among the users of the line.

This model divides the circuit cost allocation into two elements, T_1 and T_2. The first element, T_1, corresponds to the circuit current flow, i.e. the circuit capacity that is being used. Only users whose net flow is in the same direction as the line net flow, pay for this element. T_2 accounts for the additional capacity, which corresponds to the circuit reserve. Since all users benefit from this circuit reserve, all line users contribute to its cost.

$$LT^t_{DAM_k} = T^t_{1k} + T^t_{2k} \tag{7}$$

$$\begin{cases} T^t_{1_k} = |I^t_k| \sum_{l=1}^{m} \left(\dfrac{|I^t_k|}{|I^t_l|} \right) \left(\dfrac{1}{|I^t_l|^{s+}} \right) \\ \qquad \cdot CC^t_l \cdot DF^t_{lk} \quad when\ \Re\{\dot{I}^t_k/\dot{I}^t_l\} > 0 \\ T^t_{1_k} = 0 \qquad when\ \Re\left\{\dot{I}^t_k/\dot{I}^t_l\right\} \leq 0 \end{cases} \tag{8}$$

$$T^t_{2_k} = |I^t_k| \sum_{l=1}^{m} \left(\frac{|I^t_l| - |I^t_k|}{|I^t_l|} \right) \cdot \left(\frac{1}{|I^t_l|} \right) \cdot CC^t_l \cdot DF^t_{lk} \tag{9}$$

I^t_l is the sum of current flows from users in branch l at time t.

3) THE POSITIVE AMP MODEL (PAM)

The PAM allocates costs in proportion to the ratio between power flow and circuit capacity. In this model's equation, the denominator becomes circuit capacity, rather than the sum of current flows caused by all agents in each network's section. This substitution reintroduces a postage-stamp element to the tariff, preventing a situation where only line users are charged for the line circuit reserve.

As in the previous model, there is no locational charge for the agent whose current flow is in the opposite direction to the net flow. This guarantees a discount for the agent who relieves the line flow. However, this model differs in the sense that the remaining cost element is not applied on a locational basis.

The model locational tariff for bus k at time t is:

$$\begin{cases} LT_{PAM}{}^t_k = |I^t_k| \sum_{l=1}^{m} \dfrac{1}{CAP_l} CC^t_l \cdot DF^t_{lk} \quad when\ \Re\left\{\dot{I}^t_k/\dot{I}^t_l\right\} > 0 \\ LT_{PAM}{}^t_k = 0 \qquad\qquad\qquad\qquad\qquad when\ \Re\left\{\dot{I}^t_k/\dot{I}^t_l\right\} \leq 0 \end{cases} \tag{10}$$

where CAP_l is the capacity of circuit l.

The PAM does not allocate all fixed costs based on the current flow, and therefore the revenue reconciliation is formulated on the basis of each network user's contribution to the peak demand of the feeder. This is a postage-stamp type apportionment method, that is independent of the grid configuration and flow direction [12]. The postage-stamp charge, PS_k, is:

$$RCC^t = \sum_{l=1}^{m} CC^t_l \left[1 - \frac{|I^t_l|^{s+}}{CAP_l} \right] \tag{11}$$

$$PS_k = \frac{\left|I^{peak}_k\right|}{\left|I^{peak}_{total}\right|} \cdot \sum\nolimits_t RCC^t \tag{12}$$

where RCC^t is the total remaining cost at time t, I^{peak}_k is the current value in node k at peak time, and I^{peak}_{total} is the sum of current flows from users at the substation at peak time.

C. LOSS ALLOCATION

In the flow simulation, losses over 24 hours are apportioned according to consumption. The individual contribution of agents with respect to losses, is defined according to (13):

$$Loss^t_{allocation_k} = LPC^t_k \cdot Loss \cdot CC^t_{loss} \tag{13}$$

where LPC^t_k is the loss proportionality constant of the user at node k at time t. $Loss$ is the sum of all system losses calculated using the power flow method applied at a substation used as a reference bus (to this was attributed the zero reference angle). CC^t_{loss} is the system cost relating to the power losses, and:

$$\sum\nolimits_l CC^t_l + CC^t_{loss} = total\ circuit\ cost \tag{14}$$

III. CASE-STUDY

To evaluate the proposed models, we took a typical business day in June 2015 for one Brazilian distribution company. ANEEL provided the network and load data,[1] and Table 1 shows the feeder data.

Each load was formulated to be 50% constant impedance and 50% constant power, with a power factor of 0.92 for LV loads, and 0.93 for medium-voltage (MV) loads. The load-profile curves varied according to the type of consumer and were obtained by distributor survey. These are carried out

[1]The data were requested from ANEEL, in February 2019, through the website: https://www.gov.br/acessoainformacao/pt-br

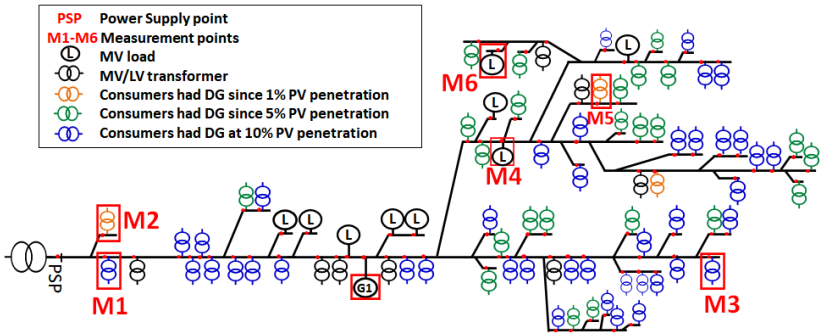

FIGURE 3. Feeder configuration.

TABLE 1. Feeder data – June/2015.

Supply voltage	13.8kV	
	Number	Installed power
Consumers in 13.8kV	9	4,689.52 kW
Consumers in 220V – industrial	14	37.95 kW
Consumers in 220V – commercial	127	239.27 kW
Consumers in 220V – residential	2,665	1,349.21 kW
Consumers in 220V – rural	0	0.00 kW
Consumers in 220V – street lighting	579	81.93 kW
Data for June/2015		
Total 220V load		21,707.24 MWh
Total 13.8kV load		67,506.84 MWh
Total load		89,214.08 MWh

every four years for the purpose of renegotiating tariffs with the regulator.

The feeder configuration and the positions of MV consumers and MV/LV transformers are shown in Fig. 3. The MV/LV transformers represent the aggregate consumption of LV consumers above them. PSP denotes the substation power supply point, G1 is the generator, and M1 to M6 are measurement points.

For simulations with DG modules, panels were dimensioned from (15), with standard 270 Wp modules for LV, and with a power factor of 1.0:

$$Pot_{solar} = \frac{Energy}{PSH \times \eta} \tag{15}$$

where, Pot_{solar} is the total solar panel power, and Energy is the total generated energy obtained by the average consumption of the unit in the last 12 months. PSH is the peak sun hours (city $=$ 4.39), and η is the panel performance (assumed to be 80%).

For the annual circuit cost, we made an annualized estimate of the value of the investment in the network by the distributor, added to the annual maintenance cost (taken to be 40% of the investment). The annual amount thus calculated is US$308,877.60.[2] The estimated useful life of the circuit was 30 years. Our intention is to define hour-by-hour separate daily tariffs, and the circuit cost is thus divided by 8,760h/year, resulting in an hourly cost for the feeder of US$35.26/h, to be allocated among the 87 consumers along the feeder.

In order to simplify the analysis, only selected buses were monitored. We chose two points with load-profile curves typical of residential LV consumers (M1 and M3 in fig. 3). To represent the MV loads, points M4 (the largest consumer) and M6 were chosen. These points are typical of industrial consumers. Finally, points M2 and M5 were selected because they are the largest LV consumers in the system and are commercial in nature.

IV. RESULTS

The proposed apportionment models – ZCAM, DAM, and PAM – were evaluated based on the net flow results. The comparison was effected using four simulations: first, hourly rate simulations without DG investors; second, hourly rate simulations with a generator located in the main branch; third, simulation with battery storage; and fourth, rate simulations with increasing percentages of DG penetration.

For the simulations, we used software written in Python, which calls the OpenDSS program.

It is important to note that our simulations are ex-ante, using consumption profiles obtained by periodical survey, and the chosen DG generation curve. However, the proposed method can also work in an ex-post approach or even in a real-time pricing application, provided there is enough available data.

A. SIMULATIONS WITHOUT DG AND ENERGY STORAGE

Without the presence of DG, current flows in the branches are unidirectional, and consequently the ZCAM and DAM models produce the same results. These are shown in Table 2, where LT ($/day) represents the locational charge results. In addition to columns for measurement points M1 to M6, two other columns are included. Column Σ_{80} gives the sum of the 80 rates for individual load buses that were not represented by the measurement points; and column Σ_{Total} gives the sum of all rates. In radial networks, this locational model calculates cumulative branch costs for each facility, and consequently, there is a significant difference between tariffs at the main branch and at the end of the feeder.

[2]US$1.00 assumed to be BRL$5.00.

TABLE 2. ZCAM/DAM charges.

	M1	M2	M3	M4	M5	M6	Σ_{80}	Σ_{total}
LT($/DAY)	0.04	6.89	15.60	88.43	11.72	44.28	654.15	**821.10**

The results in Table 2 suggest that the lack of a systematic scheme for the equitable distribution of costs within such a short feeder can either be considered an advantage, by encouraging DG investors to locate at the end of branches within the system, or as a disadvantage because it is inequitable. For example, without DG, the model without a fixed charge results in LV consumers located at M1 paying $0.0009/Ah, while others at M3, with similar residential loading (M1 load is 1.7341Ah and M3 load is 1.9900Ah), are paying $0.3266/Ah.

Table 3 shows the PAM tariffs. Here, PS ($) represents the postage-stamp element.

TABLE 3. PAM charges.

	M1	M2	M3	M4	M5	M6	Σ_{80}	Σ_{total}
LT ($)	0.02	0.05	0.44	36.59	1.08	5.47	37.96	**81.60**
PS ($)	1.20	5.48	1.48	386.42	9.08	32.02	303.82	**739.50**
Total	$							**821.10**

In general, net flow in feeders usually falls well below their maximum capacities. Therefore, the PAM needs a significant postage-stamp charge in order to recover full cost. This distorts the locational signal, although it allows for more homogeneity in tariffs. For example, M1 and M3 have similar loading and their postage-stamp charge is $1.20/day and $1.48/day respectively, whereas the locational tariff for each user is very different, at $0.02/day and $0.44/day respectively. This suggests that the PAM could provide an incentive for DG investors to locate at the end of the feeder, and that it is equitable. The locational costs on a $/Ah basis at each measurement point and illustrates that higher charges will be applied for greater distance from the substation.

The loss apportionment results obtained for the case without DG are given in Table 4, where Loss ($) represents the loss apportionment results. The sum of the tariff due to loading plus the tariff due to losses, indicates how these apportionment models cover the Utility's total daily costs of US$ 846.19/day.

TABLE 4. Loss results.

	M1	M2	M3	M4	M5	M6	Σ_{80}	Σ_{total}
LOSS($/day)	0.02	0.01	0.18	6.04	0.28	0.84	17.70	25.08

B. SIMULATIONS WITH DG AND ENERGY STORAGE

1) GENERATOR – G1

Consider the example in which ten solar panels of 100kWp each (panel efficiency is assumed to be ∼80%) are inserted into the main branch of a circuit (G1, Fig.3), resulting in the power curve described in Fig.4. In this case, the panels do not produce flow inversion in the line - i.e. their presence simply relieves the circuit flow.

With the flow direction condition (when $RI_k/I_l > 0$), the ZCAM and PAM models have zero locational charging for the generator that relieves the circuit, as shown in the $/Ah average Tables 5 and 7. Compared to the previous case – without DG – there is negligible variation in the locational tariff. The only significant difference is in PS values (Table 8), which occurs because of changes in peak time from 11:00 a.m. to 10:00 a.m.

For the DAM model, in which only part of the local tariff is subject to the flow condition, the difference between cases with and without DG is significant (Table 6). Fig.4 shows that G1 receives no ZCAM tariff, and the DAM tariff curve has the same profile as the generation curve.

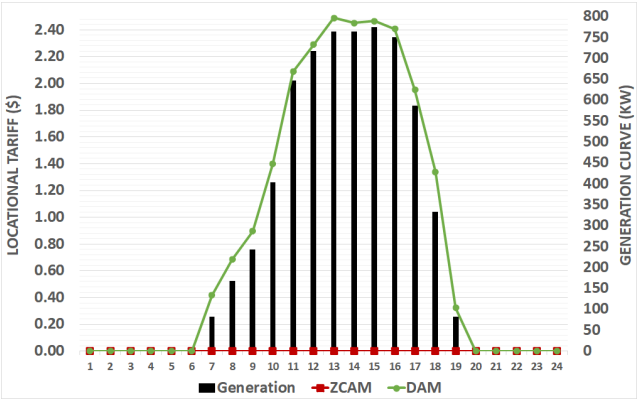

FIGURE 4. G1 total kWh generation of installed panels (kWh) and locational tariff (US$/h).

In addition, with a loss reduction from 3,161kWh in the case without DG, to 2,929kWh, the apportionment of losses generates negative charges at G1 (Table 9). This can be considered a benefit deriving from the reduction in circuit losses due to the presence of G1.

2) SIMULATION WITH STORAGE – G1

When looking at Fig. 4, it can be seen that the tariff curve has the same profile as the generation curve. If this profile extends to other sources, it is possible that any renewable or non-renewable source could be substituted in this tariff model. To verify this, we replaced the generator in G1 with a battery bank with the charge/discharge curve shown in Fig.5. The battery bank is charged in the early hours of the morning and discharged in the evening.

With the flow direction condition, the ZCAM and PAM models eliminate locational tariffs with a negative flow direction (Fig. 5). The results are shown in Tables 5 and 7. In the DAM, the total rate incorporates a flow rate and a reserve rate (Table 6). For this reason, the DAM tariff curve is always positive and follows the charge/discharge bank profile-curve (Fig.5).

The peak time in this case was at 11:00 a.m., when the battery bank was neither being charged nor discharged. The battery bank does not therefore pay PAM's postage-stamp element in this case. These results demonstrate that the presence of a postage-stamp element relating to peak time, may influence battery users to adapt their charging/discharging hours to periods when the network is less congested.

Table 9 presents the loss results. It can be seen from this that a user at G1 reduces the system loss, and this is reflected in their charges.

It is important to note that, with the presence of storage (or electric vehicles), it is desirable to send economic signals to the agent such that the charge and discharge of batteries will occur at times that will effectively attenuate the peaks and troughs of the charging curve. In order to achieve this, time-dependent differential tariffs should be applied, and all of our proposed models address this. In addition, the proposed locational rates could be used to indicate the best siting of recharging stations.

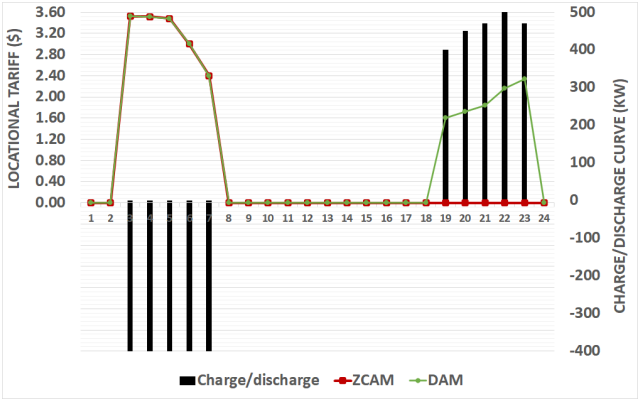

FIGURE 5. Battery bank load-profile curve and locational tariff (US/*h*).

C. SIMULATIONS WITH DG – PROSUMER

DG modules were allocated to LV consumers spread across the feeder, and Fig. 3 illustrates the location of consumers with such panels. For these simulations, a typical rooftop solar generator was attributed to LV consumers – using (15) – according to the DG penetration level. These were allocated to LV consumers in order of consumption, from highest to lowest, with panel energy output designed to match the user's energy consumption over time.

Simulations were performed at three levels of DG penetration: (a) at 1% penetration, corresponding to 254 kWp of total installed capacity. At this level, three consumers (orange in Fig. 3) had panels with a total capacity of 269 kWp installed; (b) at 5% penetration, corresponding to 1,270 kWp. At this level, seventy-five consumers (orange and blue in Fig. 3) had panels with a total capacity of 1,272 kWp installed; and, (c) at 10% penetration, corresponding to 2,540 kWp. In this case, 423 consumers (orange, blue, and green) had panels with a total capacity of 2,543 kWp installed.

1) COMPARISON OF MODELS

Tables 5 and 6 present the results for the ZCAM and DAM models. They indicate that there is little tariff variation at different penetration levels. The variations are positively correlated with the increase in penetration level and distance from the substation, but differences in tariff values are negligible.

It is important to note that, even with the presence of DG modules, the ZCAM and DAM models produced significant tariff variations between different nodes of the system with similar profiles and loading. This can be seen when comparing values from M1 and M3. As our allocation models aggregate tariffs on each branch, the tariff will be higher as the consumer moves further away from the substation. This outcome is independent of network topology.

The simulations show that the chosen flow condition (when $R\{I_k/I_l\} > 0$) correctly reflects the DG module boundaries. This can be easily seen using the ZCAM model, in which all tariff calculations are affected by the flow direction condition (unlike the other two models that have independent elements).

To illustrate this, Fig. 7 shows the current flows in the line and at the point of output from the transformer at M5. The panels are attributed to M5 customers starting from 1% of DG penetration. In this case, there is a flow inversion occurring beyond 5% of DG penetration, as shown by Fig. 6.

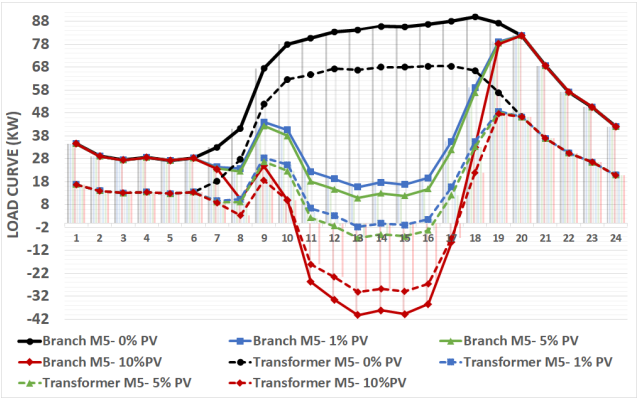

FIGURE 6. Active power flow in the M5 branch results.

The ZCAM results presented in Fig.8 show the flow inversion. At 1% penetration, the only effect of the presence of DG is to relieve the flow in the branch (Fig.6) (Fig.7a). The model therefore generates a lower tariff (compared to the case without DG) that reflects the load reduction. At 5% penetration it can be seen that the active power delivered by DG modules present in the branch, has a negative flow (Fig.6) (Fig.7b), generating a zero tariff from M5 to the power supply point (substation). Also, analyzing results at 10% penetration, where there is current inversion in the branch attributable to the DG modules (Fig.6) (Fig.7c), the model generates a charge for this inversion, but also generates a zero tariff in the upstream branches based on their load reduction.

The PAM model is similar to the previous models in the sense that its locational tariff only applies in cases where DG

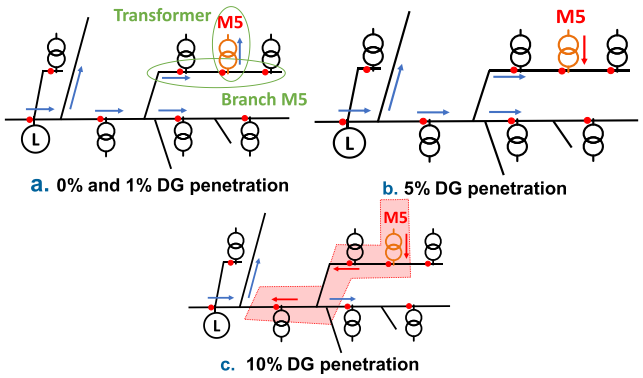

FIGURE 7. Power flow direction during daylight hours.

module current is in the same flow direction as the net flow. Tables 7 and 8 show the results.

However, the model differs in the sense that PAM has a significant residual cost value distributed according to the proportional participation of users at the peak hour of the system. Peak demand without DG occurred at 11:00 a.m. because of the industrial consumer at M4 (Fig. 9). With DG penetration, the peak hour varies, the latest time being 8:00 p.m. with 10% DG penetration.

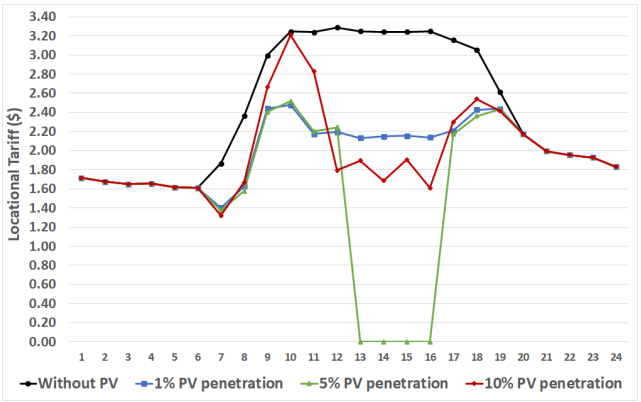

FIGURE 8. M5 ZCAM locational tariff (US/*h*).

The changes in peak time due to DG penetration benefited some users but penalized others. The user at M4 benefited from a reduction in network fixed charges when peak time moved from normal working hours to 8:00 p.m. at 10% DG penetration. Because of their solar energy input, users at M5 benefited when peak time occurred during working hours, but paid higher network charges when peak time was at night. At M1, passive residential consumers also pay more for network charges when peak time is at 8:00 p.m.

These results demonstrate that a locational tariff may influence DG investor location, while an added postage-stamp element can influence consumer consumption profiles. This suggests that a composite tariff based on both location and participation at peak load times has considerable economic signaling potential.

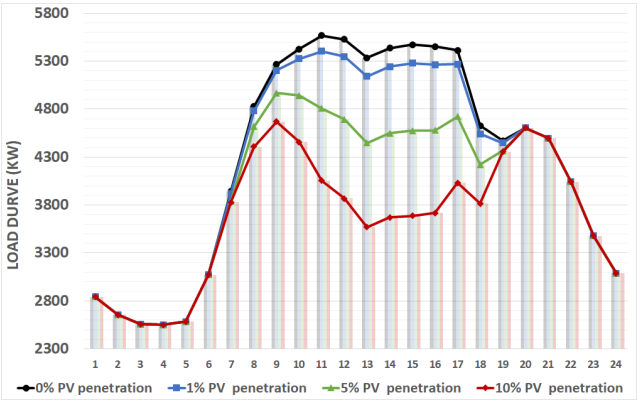

FIGURE 9. Feeder's load profile.

Finally, Table 9 shows the apportionment of loss results. With DG, system loading reduced from 102,742 kWh to 88,115 kWh with 10% DG penetration, and the loss reduced from 3,161 kWh to 2,707 kWh. In all cases, losses accounted for about 3% of the system total loading.

TABLE 5. ZCAM daily average results (US$/AH).

	LT_{ZCAM} ($/Ah)						
	M1	M2	M3	M4	M5	M6	G1
Without DG	0.0009	0.0668	0.3266	0.0134	0.0773	0.0596	-
Generator G1	0.0009	0.0668	0.3267	0.0134	0.0773	0.0596	0.0000
Battery bank G1	0.0009	0.0668	0.3264	0.0132	0.0771	0.0592	0.1293
1% DG penetration	0.0009	0.0666	0.3268	0.0135	0.0630	0.0598	-
5% DG penetration	0.0009	0.0666	0.3667	0.0138	0.0515	0.0604	-
10% DG penetration	0.0013	0.0666	0.4259	0.0141	0.0628	0.0620	-

TABLE 6. DAM daily average results (US$/AH).

	LT_{DAM} ($/Ah)						
	M1	M2	M3	M4	M5	M6	G1
Without DG	0.0009	0.0668	0.3266	0.0134	0.0773	0.0596	-
Generator G1	0.0009	0.0668	0.3265	0.0130	0.0770	0.0593	0.0053
Battery bank G1	0.0009	0.0668	0.3261	0.0130	0.0770	0.0591	0.2078
1% DG penetration	0.0009	0.0668	0.3268	0.0134	0.0625	0.0597	-
5% DG penetration	0.0009	0.0668	0.3852	0.0135	0.0582	0.0601	-
10% DG penetration	0.0012	0.0668	0.4340	0.0130	0.0638	0.0598	-

TABLE 7. PAM daily average results (US$/AH).

	LT_{PAM} ($/Ah)						
	M1	M2	M3	M4	M5	M6	G1
Without DG	0.0004	0.0004	0.0092	0.0055	0.0071	0.0074	-
Generator G1	0.0004	0.0004	0.0092	0.0055	0.0071	0.0074	0.0000
Battery bank G1	0.0004	0.0004	0.0092	0.0055	0.0071	0.0074	0.0453
1% DG penetration	0.0004	0.0003	0.0092	0.0055	0.0046	0.0074	-
5% DG penetration	0.0004	0.0003	0.0073	0.0055	0.0037	0.0074	-
10% DG penetration	0.0006	0.0003	0.0097	0.0054	0.0033	0.0074	-

V. DISCUSSION

The proposed models encompass the tariff principles of simplicity, completeness, and good economic signaling. They

TABLE 8. PAM postage stamps (US$/day).

	PS_{PAM} ($/day)						
	M1	M2	M3	M4	M5	M6	G1
Without DG	1.20	5.48	1.48	386.42	9.08	32.02	-
Generator G1	1.21	6.46	1.50	391.38	3.87	32.43	31.15
Battery bank G1	1.31	5.58	1.64	379.03	9.55	30.91	0.00
1% DG penetration	1.21	6.46	1.50	391.38	3.87	32.43	-
5% DG penetration	0.96	2.42	1.07	407.82	5.10	34.82	-
10% DG penetration	3.63	5.45	3.92	269.66	8.16	29.93	-

TABLE 9. Loss locational daily average tariffs (US$/AH).

	LOSS ($/Ah)						
	M1	M2	M3	M4	M5	M6	G1
Without DG	0.0004	0.0001	0.0039	0.0009	0.0019	0.0011	-
Generator G1	0.0004	0.0001	0.0039	0.0009	0.0019	0.0012	-0.0010
Battery bank G1	0.0004	0.0001	0.0039	0.0009	0.0019	0.0011	-0.0044
1% DG penetration	0.0004	0.0001	0.0038	0.0009	0.0030	0.0011	-
5% DG penetration	0.0004	0.0001	0.0031	0.0009	0.0015	0.0011	-
10% DG penetration	0.0006	0.0002	0.0051	0.0008	0.0018	0.0011	-

also reflect the dynamics of the load curves and the operation of DERs, as these are non-linear 24-hour load flows.

However, the ZCAM and DAM models present very different tariffs for similar consumers in different locations. This difference represents an efficient signaling mechanism where many micro- and mini-generators compete to provide energy within a radial system. Passive consumers may not be comfortable with large price differences, although this is appropriate from a distribution point of view. If necessary, the regulator could add an attenuation factor, but this would have to be acceptable to all agents.

With all the models we tested, positive-flow charges send locational signals to alternative energy investors, and provide reduced tariffs to users located in branches with a net negative flow. This is both rational and fair. However, the postage-stamp element present in the PAM may have the effect of inducing all system users to make better hourly consumption decisions.

The apportionment of circuit losses based on the sensitivity matrix sends efficient economic signals. It also follows the key principle of simplicity, and promotes the fair allocation of costs across different consumer profiles. As with the ZCAM and DAM models, the loss apportionment values are quite different between users. However, they reflect distribution network characteristics, which can penalize users far from the main transformer. Mitigating any differences should be the responsibility of the regulator, who can use policies to equalize, for instance, neighboring feeder tariffs.

VI. CONCLUSION

The paper developed and examined several models to try to determine an efficient and effective method of solving the embedded cost allocation problem in distribution networks with a high DG presence. Using AC load flow simulations in an urban feeder, we sought an optimal fixed cost allocation model across all system agents.

The proposed models seek to make a fair apportionment of infrastructure costs among network users. They differ from methods currently applied around the world because they combine time-of-use and locational signals. This logically makes them more appropriate for dealing with active distribution systems incorporating electric vehicles, batteries, DGs and other DERs.

Our work contributes to the debate over tariffs in a DER context on the following basis:

- the proposed methods match the costs to each network user based on the user's impact on the network according to the cost causality principle. They combine locational and time-of-use rates to provide effective economic signals to users. The time-of-use rates are important from a distribution point of view because peak hours are the main reason for network reinforcement and investment, and time-of-use signaling helps optimize network usage. In addition, locational rates encourage investors to install DGs far from the main substation, minimizing reinforcement and reducing losses. Earlier papers do not combine radial distribution configurations with time-of-use and locational signaling for fixed cost allocation;
- the proposed approach was developed to accommodate the relationship between node and line currents, and enables us to consider both active and reactive power simultaneously in tariff design. This is in contrast to previous work, where tariff design considered only active power, or treated active and reactive power separately;
- the proposed methods are intended to be simple and to recognize the extensive use of the distribution network by DERs. The model's positive-flow charges send locational signals to DG agents and provide reduced tariffs to users located in branches with a net negative flow. The methods are intended to be fair from a distribution point of view and provide signals for the 24-hour feeder load cycle;
- a loss sensitivity matrix based on the relationship between losses and node currents is included. This is considered important because the losses at LV and MV levels can be significant;
- finally, the proposed models are based on power flow equations that can be easily reproduced by system users and energy traders. Although the power flow equations are not simple, they are widely known and there are open-source computer programs, such as OpenDSS, that can be used by distribution companies, regulators, and also by network users.

APPENDIX
ANALITICAL DERIVATIVES CALCULATION
A. THE DERIVATIVES OF THE ABSOLUTE LINE CURRENTS WITH RESPECT TO ABSOLUTE NODE CURRENTS

We propose a new sensitivity matrix relating line and node currents. We follow the calculations from the derivatives calculation methodology in [16], but extend this to generate alternative Jacobian matrices.

The relationship between line currents and node currents in the power flow is:

$$i_k = \sum_{h \in H_k^{in}} f(h) - \sum_{h \in H_k^{out}} f(h) \tag{16}$$

where i_k is the complex charging current for node k, and f_l is the complex current flowing through line l. H_k^{in}, H_k^{out} are sets of injection points and withdrawal points in each line for respective nodes.

In the matrix form of (16) we have:

$$i = A^T \cdot f \tag{17}$$

where A is the incident matrix defined as:

$$\begin{cases} A\left(h, k_{h_{end}}\right) = 1 \\ A\left(h, k_{h_{inicial}}\right) = -1 \\ A\left(h, k\right) = 0, \quad \forall k \neq k_{h_{inicial}}, k_{h_{end}} \end{cases} \tag{18}$$

For a radial network ($n_{nodes} = n_{lines} + 1$), the slack bus, k_s, represents the power supply point where the distribution network connects to the transmission network. Then, calling i_{ns} the set of nodes other than the slack bus, the notation is now:

$$i = (i_s, i_{ns}), A = (A_s, A_{ns})$$

Thus:

$$i_s = A_s^T \cdot f \tag{19}$$

$$i_{ns} = A_{ns}^T \cdot f \tag{20}$$

Given that $i = a + jb$ and $f = c + jd$, the derivatives of the line currents with respect to node currents is:

$$c + jd = \left(A_{ns}^T\right)^{-1} \cdot (a + jb)$$

$$\frac{\partial c}{\partial a} = \frac{\partial d}{\partial b} = \left(A_{ns}^T\right)^{-1}, \quad \frac{\partial c}{\partial b} = \frac{\partial d}{\partial a} = 0$$

Then, the Jacobian matrix is:

$$J_1 = \begin{pmatrix} \frac{\partial c}{\partial a} & \frac{\partial c}{\partial b} \\ \frac{\partial d}{\partial a} & \frac{\partial d}{\partial b} \end{pmatrix} = \begin{pmatrix} \left(A_{ns}^T\right)^{-1} & 0 \\ 0 & \left(A_{ns}^T\right)^{-1} \end{pmatrix} \tag{21}$$

Now, as $F(h) = abs(f(h)) = \sqrt{c^2 + d^2}$ and $I = abs(i_k) = \sqrt{a^2 + b^2}$, then

$$J_2 = \frac{\partial F}{\partial (c, d)} = \frac{diag(c)\ diag(d)}{F} \tag{22}$$

$$J_3 = \frac{\partial I}{\partial (a, b)} = \frac{diag(a)\ diag(b)}{I} \tag{23}$$

$$(J_1) \cdot (J_2) = \left(\frac{\partial (c, d)}{\partial (a, b)}\right) \cdot \left(\frac{\partial F}{\partial (c, d)}\right) = \frac{\partial F}{\partial (a, b)} = (J_4)$$

$$(J_5) = (J_4) \cdot (J_3)^{-1} = \frac{\partial F}{\partial (a, b)} \cdot \frac{\partial (a, b)}{\partial I} \tag{24}$$

Finally, the derivatives of the absolute line currents with respect to absolute node currents are:

$$(J_5) = \frac{\partial F}{\partial I} \tag{25}$$

B. PROPORTIONALITY CONSTANT FOR THE APPORTIONMENT OF ELECTRICAL LOSSES

We determine the variation in circuit losses as follows:

The matrix form of (3):

$$P_{loss} = Re\left\{i^* . * Ri\right\} \tag{26}$$

where $i = a + jb$, the equation can be rewritten:

$$P_{loss} = Re(a - jb) . * R(a + jb)\}$$

$$P_{loss} = [a . * Ra + b . * Rb] \tag{27}$$

The derivative of a function $f(x) = u(x) .* v(x)$ is $\partial f / \partial x = diag(v) \cdot \partial u / \partial x + diag(u) \cdot \partial v / dx$. Thus,

$$J_6 = \frac{\partial P_{loss}}{\partial (a, b)} = \left(\frac{\partial P_{loss}}{\partial a} \ \frac{\partial P_{loss}}{\partial b}\right)$$

$$J_6 = = \left(diag(a)R + diag(Ra) \quad diag(b)R + diag(Rb)\right) \tag{28}$$

resulting in the derivatives of the losses with respect to absolute node currents:

$$(J_7) = (J_6) \cdot (J_3)^{-1} = \frac{\partial P_{loss}}{\partial (a, b)} \cdot \frac{\partial (a, b)}{\partial I} \tag{29}$$

REFERENCES

[1] R. Moreno, B. Bezerra, H. Rudnick, C. Suazo-Martinez, M. Carvalho, A. Navarro, C. Silva, and G. Strbac, "Distribution network rate making in Latin America: An evolving landscape," *IEEE Power Energy Mag.*, vol. 18, no. 3, pp. 33–48, May 2020.

[2] Accessed: Jul. 10, 2020. [Online]. Available: http://www.absolar.org.br/noticia/artigos-da-absolar/a-energia-solar-o-coronavirus-e-a-recuperacao-economica.html

[3] A. Faruqui and C. Bourbonnais, "The tariffs of tomorrow: Innovations in rate designs," *IEEE Power Energy Mag.*, vol. 18, no. 3, pp. 18–25, May 2020.

[4] J. Reneses and M. P. R. Ortega, "Distribution pricing: Theoretical principles and practical approaches. *IET Gener., Transmiss. Distrib.*, vol. 8, no. 10, pp. 1645–1655, 2014.

[5] M. Murali, M. S. Kumari, and M. Sydulu, "Overview of transmission pricing methods in a pool based power market," *Int. J. Adv. Sci. Eng. Technol.*, vol. 1, pp. 6–11, Jul. 2013.

[6] S. Huang, Q. Wu, S. S. Oren, R. Li, and Z. Liu, "Distribution locational marginal pricing through quadratic programming for congestion management in distribution networks," *IEEE Trans. Power Syst.*, vol. 30, no. 4, pp. 2170–2178, Jul. 2015.

[7] S. Huang and Q. Wu, "Dynamic tariff-subsidy method for PV and V2G congestion management in distribution networks," *IEEE Trans. Smart Grid*, vol. 10, no. 5, pp. 5851–5860, Sep. 2019.

[8] Z. Yuan and M. R. Hesamzadeh, "A distributed economic dispatch mechanism to implement distribution locational marginal pricing," in *Proc. Power Syst. Comput. Conf. (PSCC)*, Jun. 2018, pp. 1–7.

[9] X. Yan, C. Gu, F. Li, and Z. Wang, "LMP-based pricing for energy storage in local market to facilitate PV penetration," *IEEE Trans. Power Syst.*, vol. 33, no. 3, pp. 3373–3382, May 2018.

[10] V. Veeramsetty, V. Chintham, and D. M. V. Kumar, "Probabilistic locational marginal price computation in radial distribution system based on active power loss reduction," *IET Gener., Transmiss. Distrib.*, vol. 14, no. 12, pp. 2292–2302, Jun. 2020.

[11] A. R. Abhyankar, S. A. Soman, and S. A. Khaparde, "Min-max fairness criteria for transmission fixed cost allocation," *IEEE Trans. Power Syst.*, vol. 22, no. 4, pp. 2094–2104, Nov. 2007.

[12] I. Abdelmotteleb, T. G. S. Roman, and J. Reneses, "Distribution network cost allocation using a locational and temporal cost reflective methodology," in *Proc. Power Syst. Comput. Conf. (PSCC)*, Genoa, Italy, Jun. 2016, pp. 1–7.
[13] J. W. M. Lima, "Allocation of transmission fixed charges: An overview," *IEEE Trans. Power Syst.*, vol. 11, no. 3, pp. 1409–1418, Aug. 1996.
[14] F. Pereira, J. Soares, P. Faria, and Z. Vale, "Allocation of fixed costs considering distributed generation and distinct approaches of demand response remuneration in distribution networks," in *Proc. Clemson Univ. Power Syst. Conf. (PSC)*, Clemson, SC, USA, Mar. 2016, pp. 1–8.
[15] T. Soares, M. Cruz, and M. Matos, "Cost allocation of distribution networks in the distributed energy resources era," in *Proc. Int. Conf. Smart Energy Syst. Technol. (SEST)*, Porto, Portugal, Sep. 2019, pp. 1–6.
[16] P. M. Sotkiewicz and J. M. Vignolo, "Allocation of fixed costs in distribution networks with distributed generation," *IEEE Trans. Power Syst.*, vol. 21, no. 2, pp. 639–652, May 2006.
[17] T. Soares, P. Faria, Z. Vale, and H. Morais, "Definition of distribution network tariffs considering distribution generation and demand response," in *Proc. IEEE PES T&D Conf. Expo.*, Chicago, IL, USA, Apr. 2014, pp. 1–5.
[18] J. Bialek, "Tracing the flow of electricity," *IEE Proc.-Gener., Transmiss. Distrib.*, vol. 143, no. 4, pp. 313–320, Jul. 1996.
[19] Y. C. Chen, A. Al-Digs, and S. V. Dhople, "Mapping nodal power injections to branch flows in connected LTI electrical networks," in *Proc. IEEE Int. Symp. Circuits Syst. (ISCAS)*, May 2016, pp. 2146–2149.
[20] A. J. Conejo, F. D. Galiana, and I. Kockar, "Z-bus loss allocation," *IEEE Trans. Power Syst.*, vol. 16, no. 1, pp. 105–110, Feb. 2001.
[21] A. J. Conejo, J. Contreras, D. A. Lima, and A. Padilha-Feltrin, "Z_{bus} transmission network cost allocation," *IEEE Trans. Power Syst.*, vol. 22, no. 1, pp. 342–349, Feb. 2007.
[22] K. S. Ahmed and S. P. Karthikeyan, "Comparison of various transmission loss/cost allocation methods—A review," in *Proc. Innov. Power Adv. Comput. Technol. (i-PACT)*, Apr. 2017, pp. 1–4.
[23] R. Bhakar, V. S. Sriram, N. P. Padhy, and H. O. Gupta, "Cost allocation of DG embedded distribution system by game theoretic models," in *Proc. IEEE Power Energy Soc. Gen. Meeting*, Calgary, AB, Canada, Jul. 2009, pp. 1–7.
[24] P. Pediaditis, D. Papadaskalopoulos, A. Papavasiliou, and N. Hatziargyriou, "Bilevel optimization model for the design of distribution use-of-system tariffs," *IEEE Access*, vol. 9, pp. 132928–132939, 2021, doi: 10.1109/ACCESS.2021.3114768.
[25] R. C. Dugan and T. E. McDermott, "An open source platform for collaborating on smart grid research," in *Proc. IEEE Power Energy Soc. Gen. Meeting*, Detroit, MI, USA, Jul. 2011, pp. 1–7.

VERONICA S. ETCHEBEHERE received the B.Sc. and M.Sc. degrees in electrical engineering from the Universidade Federal de Itajubá (UNIFEI/MG), Brazil, in 2010 and 2014, respectively, where she is currently pursuing the D.Sc. degree in electrical engineering.

Since 2015, she has been an Assistant Professor with the Universidade Federal do Amazonas (UFAM/AM), Brazil. In 2012, she has worked as a Accounting Analyst with the Brazilian Energy Trading Chamber (CCEE), São Paulo, Brazil. Her research interests include energy markets, electricity tariff structure, and power system regulation.

JOSÉ W. MARANGON LIMA (Senior Member, IEEE) received the B.Sc. degree in electrical engineering from the Instituto Militar de Engenharia (IME/RJ), in 1979, the B.Sc. degree in business administration from the Universidade Federal do Rio de Janeiro (UFRJ/RJ), in 1980, the M.Sc. degree in electrical engineering from the Universidade Federal de Itajubá (UNIFEI/MG), and the D.Sc. degree in electrical engineering from the UFRJ/RJ, in 1994.

He was a Professor of electrical engineering with UNIFEI/MG, from 1993 to 2015. In his sabbatical year (2005), he studied with the Operations Research Department, The University of Texas, USA. From 2012 to 2015, he was a Provost for Extension at UNIFEI. From 1980 to 1993, he has worked with Eletrobrás, the public power company, where he participated in and coordinated studies on power system operations and planning. He was an Advisor to the board with ANEEL, the Brazilian National Regulatory Agency, from 1998 to 1999. At the Brazilian Ministry of Mines and Energy, he was a Coordinator of the Price and Tariff Technical Committee, in 2001, and, in 2003, was a member of the group that elaborated the New Brazilian Electricity Model. He is currently a Senior Consultant at MC&E. He is the author and a coauthor of more than 150 published articles on energy, regulation and power systems operation and planning. He has been a consultant and lectured for more than 20 companies.

Dr. Marangon Lima is a Senior Member of Cigré.